Open access • Journal Article • DOI:10.1103/PHYSREVB.89.035435

Subwavelength waveguides composed of dielectric nanoparticles — Source link

Roman S. Savelev, Alexey P. Slobozhanyuk, Andrey E. Miroshnichenko, Yuri S. Kivshar ...+1 more authors

Institutions: Australian National University

Published on: 30 Jan 2014 - Physical Review B (American Physical Society)

Topics: Dielectric, Dispersion (optics) and Electromagnetic radiation

Subwavelength waveguides composed of dielectric nanoparticles

Roman S. Savelev,[1] Alexey P. Slobozhanyuk,[1] Andrey E. Miroshnichenko,[2] Yuri S. Kivshar,[1,2] and Pavel A. Belov[1]
[1]*National Research University of Information Technologies, Mechanics and Optics (ITMO), St. Petersburg 197101, Russia*
[2]*Nonlinear Physics Centre, Research School of Physics and Engineering, Australian National University, Canberra, Australian Capital Territory 0200, Australia*

(Received 28 October 2013; revised manuscript received 23 December 2013; published 30 January 2014)

We study waveguiding of the electromagnetic energy below the diffraction limit with arrays of dielectric nanoparticles through the excitation of both electric and magnetic Mie resonances. We analyze the dispersion characteristics of such coupled-resonator optical waveguides by means of the coupled-dipole approximation and then verify the validity of the coupled-dipole model by comparing the results with direct numerical simulations. We reveal that a chain of silicon nanoparticles with realistic material losses can guide light for the distances exceeding several tens of micrometers, which is significantly better than the guiding by any plasmonic waveguide with the propagation distances less than 1 μm. We verify the main concept and our theoretical findings experimentally at microwaves for an array of ceramic particles.

DOI: 10.1103/PhysRevB.89.035435 PACS number(s): 41.20.Jb, 42.25.−p, 42.82.Et

I. INTRODUCTION

A new type of optical waveguide, drastically different from conventional waveguides involving either the Bragg scattering or total internal reflection, is based on the guiding properties of an array of coupled high-Q optical resonators [1]. Recent realizations of such novel waveguides include chains of microresonators or microcavities [2–4], magnetoinductive waveguides [5–11] with magnetic resonators coupled by induced voltages, and chains of metallic nanoparticles with subwavelength localized waves guided due to the excitation of surface plasmon polaritons [12–28]. Very small sizes of plasmonic nanoparticles and the ability of such waveguides to bend without any significant reduction of a signal propagation suggest their use as building blocks for photonic integrated circuits [14]. Conventionally, a nanoparticle waveguide can be modeled as an infinite chain of magnetic or electric dipoles, and it supports guided waves under certain conditions when losses are neglected [20,29]. It was demonstrated that the propagation constants of plasmonic modes are strongly affected by nonquasistatic components of the dipole field and the effect of retardation in polarizability and mainly by dissipative losses in metals [19]. Experimental plasmonic chains were studied in Refs. [15,16,30–32], where limited propagation distances of optical signals were observed. In order to decrease the signal attenuation, one can employ core-shell plasmonic nanoparticles [33], adjust a design of the waveguiding structures [24,27,34], or introduce gain media [35–37]. However, all such advances do not allow achieving substantially longer propagation distances of the guided modes, and therefore this limits applications of plasmonic waveguides based on metal nanoparticles.

One of the approaches that can improve the propagation distances of optical energy in array waveguides is to use dielectric nanoparticles with high refractive index, such as silicon. According to the Mie solutions, silicon spherical subwavelength nanoparticles can support both magnetic dipole (MD) and electric dipole (ED) resonances in the optical frequency range [38]. Such a feature of dielectric particles, i.e., the presence of both magnetic and electric resonances, gives an additional control possibility over the light scattering. It has been employed to improve efficiency of optical nanoantennas [39,40] and achieve all-dielectric negative-index metamaterials at mid-IR [41] (experimentally shown in [42]) and optical frequencies [43]. For a silicon nanoparticle with the refractive index $n \approx 4$ and radius $R \approx 100$–200 nm, the lowest frequency resonance is the MD resonance at wavelength $\lambda_m \approx 2nR$, which makes the linear size of particles several times less than the operating wavelength. Recently, those resonances were experimentally demonstrated [44,45]. From a practical point of view, silicon photonics is considered to be very promising for the development of optical and optoelectronic photonic integrated circuits [46,47] because of a possible use of silicon microelectronics fabrication technologies. The most important advantages of dielectric particles over plasmonic ones, when it comes to the waveguide applications, is the level of losses, which is several times lower in silicon than in metals.

One-dimensional arrays of dielectric nanoparticles were studied for the subwavelength guiding in a number of papers [48–59]. In particular, Quidant *et al.* [48] demonstrated numerically and experimentally the possibility of using a chain of mesoscopic dielectric (TiO_2) heterowires as a subwavelength waveguide with the propagation distances of several micrometers. In other studies [53,55], it was shown numerically that a chain of infinitely long circular GaAs rods with radius 100 nm (below the diffraction limit) and a chain of appropriately arranged dielectric nanospheres with high refractive index allow the energy transfer with a subwavelength transverse confinement and also that propagating signals can be transported around corners and split with Y-type structures. The possibility of bending periodic dielectric waveguides at the angles up to 180° with high efficiency was numerically demonstrated in Refs. [49,51,54]. Some features (in particular, high quality factors) of the wave propagation in finite chains of dielectric particles were demonstrated [50,52]. Although the use of dielectric particles imposes a low limit on the particles size (while plasmonic particles of any size support plasmonic resonance), all studies claimed a much higher propagation distances in dielectric chain waveguides compared to plasmonic arrays. A consistent theory based on a dipole approximation,

which makes it possible to study the dispersion characteristics of complex dipolar waves in one-, two-, and three-dimensional arrays of electric and/or MDs, was developed in Refs. [57,58].

In this paper, we employ a theoretical approach to study the transmission properties of one-dimensional chains of silicon nanoparticles, which under certain conditions can be modeled as an array of electric and magnetic dipoles. To characterize the guiding properties and justify the applicability of the model, we compare theoretical results with numerical simulations. Furthermore, we verify experimentally the concept of subwavelength waveguides composed of dielectric particles in the radio-frequency range. We also estimate the propagation distances in such waveguides depending on the particle spacing and radius.

The paper is organized as follows. In Sec. II, we introduce our theoretical model that describes an array of coupled electric and MDs, and then verify it in Sec. III with direct numerical simulations. Our experimental results are summarized in Sec. IV, and then Sec. V concludes the paper. We note that the Gaussian system of units is used in all equations throughout the paper.

II. THEORETICAL MODEL

We start our study by describing a coupled-dipole approximation model [38,60,61], which we employ to obtain the dispersion characteristics of a chain of silicon nanoparticles shown schematically in Fig. 1(a). Silicon particles of radius R with refractive index n are simulated as magnetic and electric point dipoles with magnetic $\mathbf{m}$ and electric $\mathbf{p}$ momenta, oscillating with frequency ω [$\propto\exp(-i\omega t)$]. For the zeroth point dipole the momenta induced by the electromagnetic field of all other dipoles in the chain can be written in as

$$\mathbf{p}_0 = \alpha_e \sum_{n\neq 0} (\widehat{C}_n \mathbf{p}_n - \widehat{G}_n \mathbf{m}_n),$$

$$\mathbf{m}_0 = \alpha_m \sum_{n\neq 0} (\widehat{C}_n \mathbf{m}_n + \widehat{G}_n \mathbf{p}_n),$$

where $\widehat{C}_n = A_n \widehat{I} + B_n(\hat{\mathbf{r}}_n \otimes \hat{\mathbf{r}}_n)$, $\widehat{G}_n = -D_n \hat{\mathbf{r}}_n \times \widehat{I}$, $\otimes$ is a dyadic product, $\widehat{I}$ is the unit 3×3 tensor, $\hat{\mathbf{r}}_n$ is the unit vector

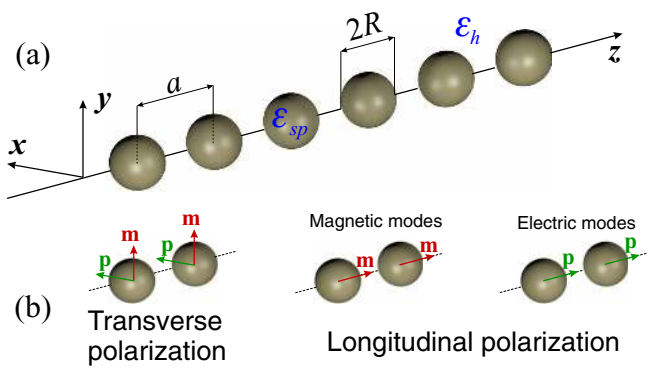

FIG. 1. (Color online) (a) A chain of dielectric (with permittivity ε_{sp}) particles with radius R and period a, located in the host medium with permittivity ε_h. (b) Schematic of all different eigenmodes in a chain of nanoparticles.

in the direction from the zeroth to the nth sphere, and

$$A_n = \frac{\exp(ik_h a|n|)}{a|n|}\left[k_h^2 - \frac{1}{(a|n|)^2} + \frac{ik_h}{a|n|}\right],$$

$$B_n = \frac{\exp(ik_h a|n|)}{a|n|}\left[-k_h^2 + \frac{3}{(a|n|)^2} - \frac{3ik_h}{a|n|}\right],$$

$$D_n = \frac{\exp(ik_h a|n|)}{a|n|}\left(k_h^2 + \frac{ik_h}{a|n|}\right),$$

where $a|n|$ is the distance between the centers of the zeroth and the nth spheres, a is the period of the structure, ε_h is the permittivity of the host medium, and $k_h = \sqrt{\varepsilon_h}\omega/c$ is the host wave number.

Knowing the magnetic and electric polarizabilities α_m and α_e of the sphere, we can obtain three independent dispersion equations [20,57,58]. The first equation is for the transverse polarization [see Fig. 1(b)],

$$\left(\frac{a^3}{\alpha_e} - A\right)\left(\frac{a^3}{\alpha_m} - A\right) - D^2 = 0, \tag{1}$$

and two other equations describe the longitudinal polarization [see Fig. 1(b)],

$$\frac{a^3}{\alpha_m} - (A + B) = 0, \tag{2}$$

$$\frac{a^3}{\alpha_e} - (A + B) = 0, \tag{3}$$

where

$$A = a^3 \sum_{n\neq 0} A_n e^{i\beta an} = (k_h a)^2 \mathrm{Li}_1^+ + ik_h a \mathrm{Li}_2^+ - \mathrm{Li}_3^+,$$

$$D = a^3 \sum_{n\neq 0} \frac{|n|}{n} D_n e^{i\beta an} = (k_h a)^2 \mathrm{Li}_1^- + ik_h a \mathrm{Li}_2^-,$$

$$B = a^3 \sum_{n\neq 0} B_n e^{i\beta an} = 3\mathrm{Li}_3^+ - 3ik_h a \mathrm{Li}_2^+ - (k_h a)^2 \mathrm{Li}_1^+,$$

$$\mathrm{Li}_s^\pm = \mathrm{Li}_s\{\exp[i(k_h + \beta)a]\} \pm \mathrm{Li}_s\{\exp[i(k_h - \beta)a]\},$$

with the function $\mathrm{Li}_s(z) = \sum_{k=1}^{\infty} \frac{z^k}{k^s}$ as a common polylogarithm [62]; here β is the Bloch wave number, and

$$\frac{1}{\alpha_e} = -i\frac{2k_h^3}{3\varepsilon_h a_1^{sc}}, \quad \frac{1}{\alpha_m} = -i\frac{2k_h^3}{3b_1^{sc}}, \tag{4}$$

are the inverse electric and magnetic polarizabilities, respectively, defined from the Mie theory [63], with a_1^{sc} and b_1^{sc} being the scattering coefficients.

In our calculations, we choose the following parameters: permittivity of silicon particles $\varepsilon_{sp} = 16$, permittivity of the host medium $\varepsilon_h = 1$, radius of the particle $R = 70$ nm. Two values of period a are considered: $a = 2R = 140$ nm, when particles are touching each other, and $a = 200$ nm. We do not take into account the material dispersion of silicon because the real part of the permittivity does not change significantly in the required spectral range and the imaginary part is small enough, so the changes caused by material losses would be proportional to $\mathrm{Im}(\varepsilon_{sp})$ and therefore can be easily evaluated, being small. In the optical frequency range, $\mathrm{Im}(\varepsilon_{sp})$ can be as

small as ≈0.05 and even being several times smaller in the near-infrared region [64].

III. NUMERICAL RESULTS

First, we study the characteristics of guided waves in chains of lossless silicon particles. The imaginary part of inverse polarizabilities (4) for the lossless spheres in the transparent medium are [65]

$$\mathrm{Im}(1/\alpha_e) = -i\frac{2}{3}\frac{k_h^3}{\varepsilon_h}, \quad \mathrm{Im}(1/\alpha_m) = -i\frac{2}{3}k_h^3,$$

so that the left-hand sides of the dispersion equations (1)–(3) for real-valued $\beta > k_h$ are also real valued [57], thus providing the conditions for existence of allowed bands with unattenuated guided modes near the MD and ED resonances. This is the property of an infinite chain of lossless scatterers. For any finite-size chain dispersion, equations (1)–(3) would be complex valued and the modes would be attenuated due to radiative losses, i.e., scattering in the free space.

Real-valued solutions are obtained by solving analytical dispersion equations for the periods $a = 200$ nm and $a = 140$ nm, and they are shown in Figs. 2(a) and 2(b). Two solid curves correspond to the transversely polarized forward waves marked as TM and TE. The abbreviation TM (or TE) does not mean that this transverse eigenmode is purely magnetic (electric) mode, i.e., a mode of a chain of magnetic (electric) dipoles; rather it means that an allowed TM (TE) band is close to MD (ED) resonance of a silicon particle. We also show the dispersion curves for noninteracting chains of magnetic and electric dipoles, i.e., when an electric moment vanishes (purely magnetic transverse-polarized modes, marked with MD) and when a magnetic moment vanishes (purely electric transversely polarized modes, marked with ED), obtained with

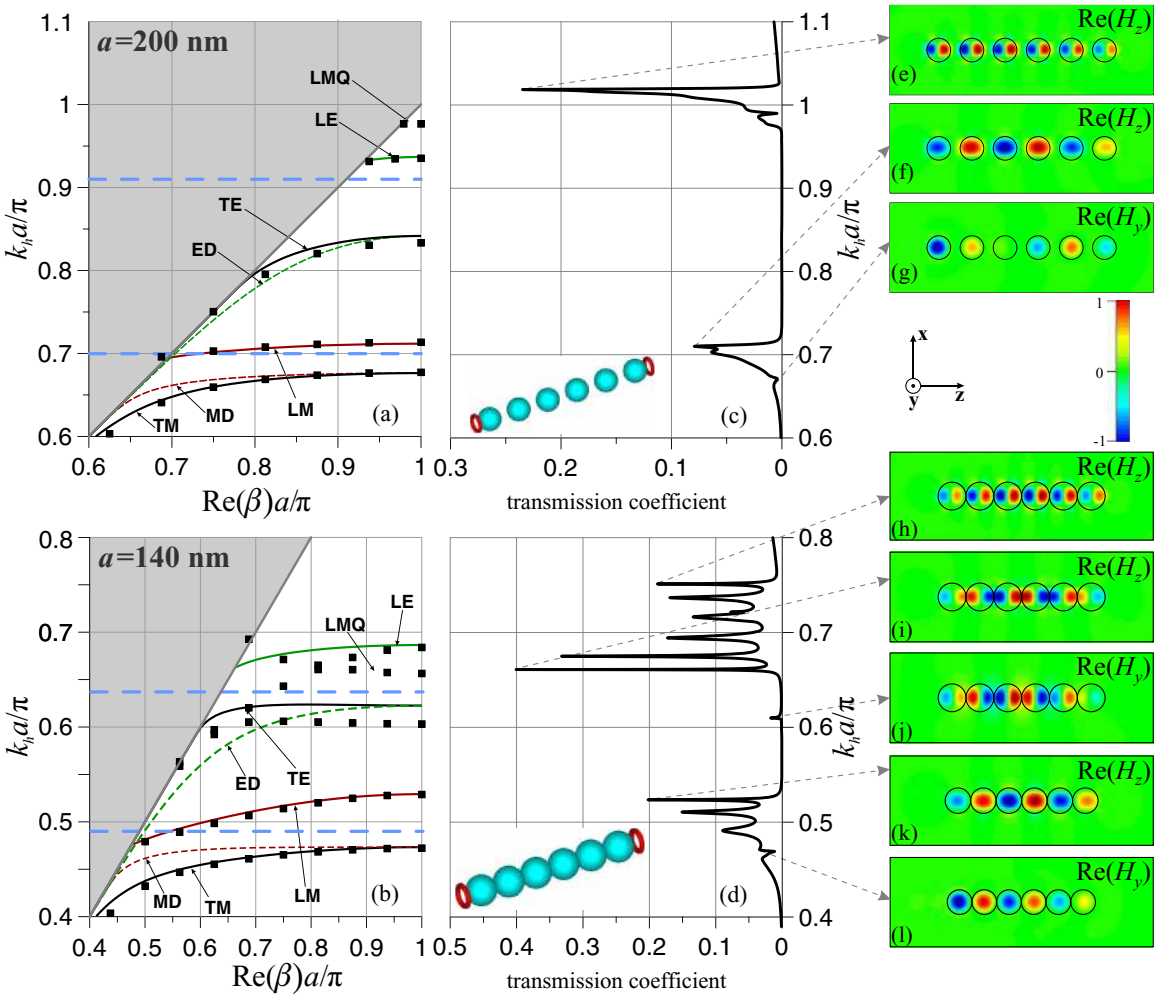

FIG. 2. (Color online) (a),(b) Dispersion diagrams of infinite chains of lossless spherical silicon nanoparticles and uncoupled chains of electric and magnetic dipoles (only real solutions of dispersion equations for both transverse and longitudinal polarizations are shown) for period of (a) 200 nm and (b) 140 nm. Solid black curves (TM and TE) show solutions of Eq. (1), dashed curves (MD and ED) show solutions of Eqs. (5), solid red and green curves (LM and LE, respectively) show solutions of Eqs. (2) and (3). Eigenmodes, numerically calculated with the MPB package, are shown with black squares. The oblique gray line is the light line. Horizontal dashed blue lines indicate the positions of MD and ED resonance frequencies. (c),(d) Numerically calculated transmission spectra of a chain of six silicon spheres with periods (c) $a = 200$ mm and (d) $a = 140$ nm. (e)–(l) Electric field distributions in the corresponding modes. The operational range of normalized frequenices $k_h a/\pi$ lies within an optical spectral range for the chosen values of period.

the following dispersion equations:

$$\frac{a^3}{\alpha_m} - A = 0, \quad \frac{a^3}{\alpha_e} - A = 0. \tag{5}$$

In contrast to the transversely polarized modes, for the longitudinally polarized modes there is no coupling between magnetic and electric dipoles, so that both red and green curves marked with LM and LE are solutions of the independent dispersion equations (2) and (3), respectively.

Following from Fig. 2(a), for large-enough periods ($a \gtrsim 3R$) the modes TM and MD and TE and ED almost coincide, because MD and ED resonance frequencies of silicon spheres with chosen parameters are located far from each other and, therefore, the magnetic and EDs are weakly interacting with each other. One of the transversely polarized modes—the TM mode—is almost completely a magnetic mode, and another—TE—is almost completely electric. In Fig. 2(b), when the gap between the particles is absent, the difference in the dispersion curves becomes substantial, which emphasizes the necessity of consideration of both magnetic and electric modes simultaneously, especially for the chains of smaller periods.

To determine the conditions under which the dipole approximation model remains valid, in Figs. 2(a) and 2(b) we compare the results obtained with the analytical model with the numerical results shown with black squares, calculated using the MPB package [66]. This approach employs the supercell method, so, in principle, we calculate eigenmodes of a three-dimensional array, but with large periods in both x and y directions. It is a reasonable approximation for a one-dimensional array, when the field is well confined in the transverse directions, i.e., when $r_{\text{loc}} = 1/[2\text{Im}(k_r)]$ is small, where $k_r = \sqrt{k_h^2 - \beta^2}$. Therefore, near the light line ($\beta = k_h$) there might be a certain inaccuracy in the MPB calculations.

Two numerically found low-frequency guided TM and LM modes coincide exactly with the modes described by the analytical model for both periods. Electric transverse TE and longitudinal LE modes are well described by the dipole model, when there exists a large-enough gap between the spheres, but when the gap vanishes, the dipole model exhibits a small inaccuracy near the ED resonance [Fig. 2(b)]. The similar difference between the dipole model and exact solutions, obtained by summation of all multipole moments, for the TE and LE modes was also reported in Ref. [59] for a chain of dielectric spheres with permittivity $\varepsilon = 10$.

Numerical calculations also indicate the excitation of higher-order multipole modes, absent in the dipole model. The magnetic quadrupole (MQ) resonance frequency of a silicon sphere is higher than the ED resonance frequency [67], but the corresponding longitudinal magnetic quadrupole (LMQ) band broadens, when the period of chain decreases, shifting partially to lower frequencies [Fig. 2(b)], thus making the dipole approximation incomplete near the ED resonance frequency for very small periods. Other multipole modes remain at higher frequencies, and we do not show them in Fig. 2. Thus, unlike the plasmonic chain waveguides, where the field is strongly localized in gaps between the particles, and the multipole approach is deemed to be necessary even for the large periods [68–70], eigenmodes of a silicon chain waveguide can be very accurately described within a dipole approximation in a wide range of parameters.

To study the realistic case of chains of a finite extent and to check a possibility of exciting the numerically found eigenmodes, we employ CST Microwave studio [71] for simulating the transmission of optical signals generated by a magnetic loop probe through two chains of six silicon spheres with 200- and 140-nm periods [Figs. 2(c) and 2(d)], respectively. Magnetic loop probes, oriented along the chain, are located on both ends of the chain as a source and receiver of radiation. Due to the inhomogeneity of current in these probes, not only LM and LMQ, but also TM and even TE modes (in the case of touching spheres) are excited.

For a chain with a 200-nm period [Fig. 2(c)] we clearly observe a transmission band around $k_h a/\pi = 0.7$ formed by excited TM and LM modes [Figs. 2(f) and 2(g)]. A transmission band around $k_h a/\pi = 1$ is formed by multipole modes. The highest peak corresponds to the LMQ mode with $\beta = 0$ [Fig. 2(e)], which is excited more effectively than other modes. This mode crosses the light line (i.e., this is a radiating leaky wave), and therefore it is not shown in Fig. 2(a), where only unattenuated modes are presented. The same situation is observed in Figs. 2(b) and 2(d) for the chain with the period of 140 nm. To calculate these frequencies (at the upper edges of the LMQ bands), we use the eigenmode solver in CST Microwave Studio. We place the chains in a 700×700 nm rectangular waveguide with PEC walls, so energy is conserved, and because the modes are longitudinal, we are able to track them distinctly for any Bloch wave number β. Numerically found frequencies for $\beta = 0$ are $k_h a/\pi \approx 1.02$ for a 200-nm period and $k_h a/\pi \approx 0.76$ for a 140-nm period, which coincide with the values in the transmission spectra at the upper edges of the LMQ bands [Figs. 2(e) and 2(h)].

For the chain with the period of 140 the transmission peaks correspond to LMQ [Figs. 2(h) and 2(i)], LM [Fig. 2(k)], and TM [Fig. 2(l)] modes, which are consistent with the calculated dispersion curves. It is known [72], that the magnetic resonance of such spheres is strongly localized within them, so the spheres are coupled stronger, and LM and LMQ bands become wider, when the period of the chain decreases [5]. One can also observe a transmission peak at $k_h a/\pi \approx 0.61$ [Fig. 2(j)] corresponding to the TE mode, which is also excited due to the current inhomogeneity in the probes.

Within a dipole approximation, our analytical model makes it possible to calculate leaky waves, which we observe in the CST simulation, and to take into account losses in silicon. Figure 3 presents a more general case of Fig. 2(a) that includes complex solutions (leaky waves). We show the dispersion diagrams in the case of only transversely polarized modes for the chain of (a) and (b) lossless and (c) and (d) absorptive silicon particles with the period of 200 nm (the case of the 140-nm period is qualitatively similar). Modes 1 and 2 and the corresponding modes in the uncoupled model (and their symmetric counterparts in the lossless case) are analytical continuations of the modes TM, MD, TE, and ED in Fig. 2(a). We observe that interaction between magnetic and electric dipoles affects mostly the leaky waves [$\text{Im}(\beta) > 0$]. Modes 1 and 2 (as well as modes 3 and 4) that start as purely magnetic and electric modes are well described only at very low frequencies, while at higher frequencies, close to the resonances of the

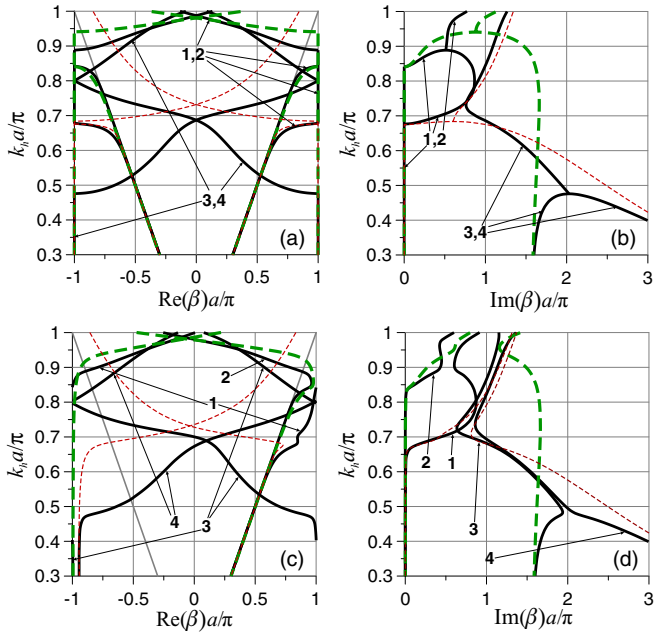

FIG. 3. (Color online) Structure of complex modes for the chain of (a),(b) lossless and (c),(d) lossy silicon spheres with period of 200 nm. Solid black lines show solutions of Eq. (1), short-dashed red and long-dashed green lines show dispersion curves of the chains of purely electric and purely magnetic dipoles, respectively, described by Eqs. (5).

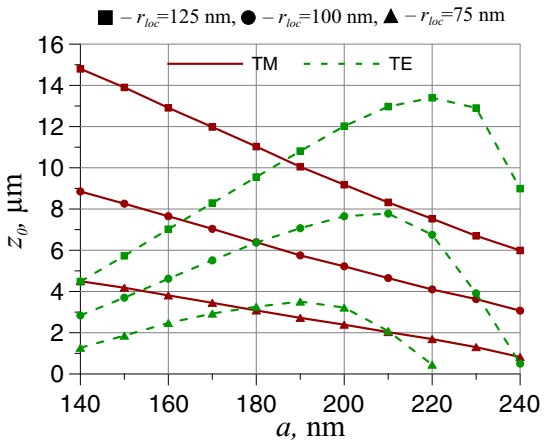

FIG. 4. (Color online) Propagation distance z_0 as a function of the period a of the chain for three different radii of localization $r_{\rm loc}$ for transversely polarized modes. Red solid curves correspond to the "magnetic" TM modes; green dashed curves correspond to the "electric" TE modes.

sphere, they merge into an indistinguishable branch that is substantially different from the modes of independent MDs and EDs chains. Meanwhile, the guided modes with $\mathrm{Im}(\beta) = 0$ undergo a slight change, as shown in Fig. 2(a). Besides the common interest of the entire complex mode structure of such chains, dispersion characteristics of the leaky waves might be of special importance for optical nanoantennas based on periodic arrays of small scatterers [39,73].

In the case of lossy silicon spheres [Fig. 3(b)] with $\mathrm{Im}(\varepsilon_{sp}) = 0.5$ (we choose a large value 0.5, so the difference in the mode structure caused by losses could be easier traced) degenerated modes 1,2 and 3,4 split, and the system does not have symmetric β and β^* solutions. Interaction between MDs and EDs affects the real parts of guided modes 1 and 2 even more, when the material losses are taken into account.

Numerical calculations of complex modes allow us to estimate such important characteristics of waveguides as a balance between the propagation distance $z_0 = 1/[2\mathrm{Im}(\beta)]$ and the field localization in the transverse direction $r_{\rm loc}$. In Fig. 4, we show the dependencies of z_0 on the period of the structure for three different values of $r_{\rm loc}$: 75, 100, and 125 nm. We observe that the propagation distance for the TM mode grows with decreasing the chain period, reaching the maximum value $z_0 \approx 15$ μm (for $r_{\rm loc} = 125$ nm), when the period equals two radii. TM modes are well described within a dipole model, so such estimates can be considered as pretty accurate. A TE mode with some fixed value of $r_{\rm loc}$ has the maximum propagation distance z_0 at a certain value of period. This value z_0 is approximately the same as that for the TM mode with the same radius of localization $r_{\rm loc}$.

The estimates of the propagation distances are made for the level of losses $\mathrm{Im}(\varepsilon_{sp}) = 0.1$ corresponding to the wavelength $\lambda \approx 700$ nm. In the spectral range 700–1000 nm losses can be several tens of times less [64], and therefore the propagation distances can reach tens and even hundreds micrometers, while the radius of the field localization would be considerably less than the operating wavelength. Comparison to the nanowaveguides, based on plasmonic particles, where the propagation distances are predicted to be several hundred nanometers [12,16], about 2 μm for the core-shell particles chains [33] and up to 10 μm for multiple-particle chains [74,75], indicates the apparent advantage of the waveguides composed of dielectric nanoparticles, so that the propagation lengths more than 10 μm can be achieved with silicon nanospheres even at the frequencies where losses are rather strong for bulk dielectric material.

IV. CONCEPTUAL EXPERIMENTAL VERIFICATION AT MICROWAVES

In order to verify experimentally the concept of a dielectric waveguide composed of a chain of dielectric nanoparticles, we scale down the dimensions to the microwave frequency range. To mimic the silicon spheres at these frequencies, we employ MgO-TiO_2 ceramic particles characterized by dielectric constant of $\approx$15.4 and dielectric loss factor of $\approx 1.15 \times 10^{-4}$ measured in the 4–10-GHz frequency range.

The experimental structure consists of six ceramic spheres with radius $R_c \approx 7.5$ mm, placed with periods $a \approx R_c(200/70) \approx 21.4$ mm [Fig. 5(a)] and $a \approx R_c(140/70) = 15$ mm [Fig. 5(b)]. Particles are located on a substrate made of a styrofoam material with the dielectric permittivity of 1. The experimental setup consists of two small (6 and 8 mm inner diameter) shielded-loop antennas, which are connected to the vector network analyzer (Agilent E8362C) through coaxial cables (85131F). The transmitting loop antenna is located 1 mm in front of spheres and the receiving antenna 1 mm behind the spheres in such a way that magnetic moments are oriented along the spheres (in the z direction). In such a configuration,

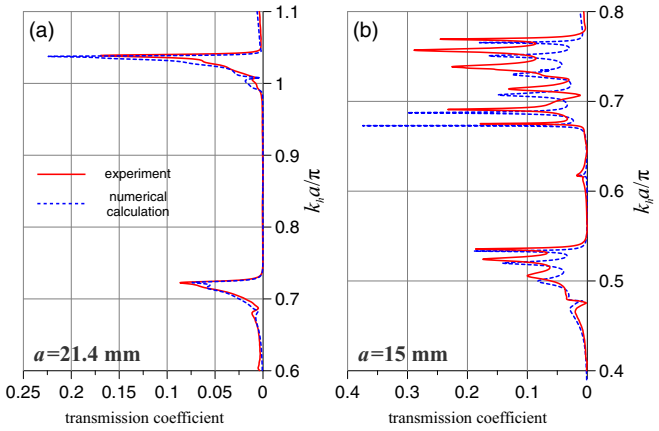

FIG. 5. (Color online) Comparison between experimental data (solid red curves) and numerically calculated transmission spectra (dashed blue curves) for a chain of six ceramic spheres with radius $R_c = 7.5$ mm, $\varepsilon_c = 15.4$, and periods (a) $a = 21.4$ mm and (b) $a = 15$ mm.

the experimental setup is similar to that employed for the measuring magnetoinductive waveguides, which support only LM modes. In our case, excitation sources are not ideal magnetic point dipoles, so the modes of different types are excited. Due to an inefficient coupling between loop antennas and chain-waveguide modes, the transmission coefficients are well below the unity. An analysis of various methods of effective excitation of a certain eigenmode requires a more rigorous approach, and it is a subject of a separate different study.

As is explained above, for the chain with nonzero gap [Fig. 5(a)] we observe rather narrow LM and LMQ bands with one sharp peak in each band. In the case of touching spheres [Fig. 5(b)] these bands broaden and six distinct peaks (at least for a LMQ band) are observed. Besides, low-transmission peaks at the frequencies $k_h a/\pi \approx 0.47$ and $k_h a/\pi \approx 0.62$ indicate that the excitation of TM and TE modes [see Figs. 2(j) and 2(l)] is also possible. Both experimental spectra in Figs. 5(a) and 5(b) show very good agreement with numerical simulations, which are performed with the help of CST Microwave Studio. Therefore, experimental results prove a possibility of using a chain of dielectric particles as a waveguide with the subwavelength energy localization, which may be a very good alternative to the chains of plasmonic nanoparticles.

V. CONCLUSIONS

We have analyzed the dispersion properties of arrays of silicon nanoparticles with different periods. We have shown that such nanoparticle arrays create subwavelength waveguides that support MD, ED, and MQ guided modes with reasonable propagation distances and subwavelength energy localization. A comparison with numerical simulations indicates that the coupled-dipole model describes very accurately MD modes, and it remains valid for ED modes in the case of large spacing. For small lattice spacings, MQ mode shifts to lower frequencies, and the dipole model gives inaccurate predictions at the frequencies near the ED resonance. More accurate description requires to take into account also the MQ moment.

We emphasize that for the analysis of the guided modes in a chain of silicon particles it is necessary taking into account both magnetic and electric moments. Interaction between the EDs and MDs affects strongly the dispersion characteristics of leaky waves and also guided waves, when the lattice spacing becomes small.

Our analytical and numerical results, also verified by microwave experiments, indicate many advantages of chains of silicon nanoparticles over plasmonic arrays and confirm a promising perspective of using them as waveguides with subwavelength guiding in optical integrated circuits.

One of the important issues for the further study is the influence of the surrounding medium on the guiding properties of such chains. For the mostly confined modes one does not expect any significant differences, because the field in these modes is strongly localized inside the particles. However, in certain practically important cases, especially when a chain lies right on a substrate, it may substantially affect its guiding properties [23,28,76].

ACKNOWLEDGMENTS

The authors acknowledge useful discussions with I. Shadrivov and thank E. Nenasheva for providing the ceramic particles. This work was supported by the Ministry of Education and Science of the Russian Federation (Grant No. 11.G34.31.0020), the Government of Russian Federation, Grant No. 074-U01, by RFBR Project No. 14-02-31761, Grant of the President of the Russian Federation, the Dynasty Foundation, and the Australian Research Council via Future Fellowship Program (FT110100037).

[1] A. Yariv, Y. Xu, R. K. Lee, and A. Scherer, Opt. Lett. **24**, 711 (1999).
[2] S. Deng, W. Cai, and V. N. Astratov, Opt. Express **12**, 6468 (2004).
[3] Z. Chen, A. Taflove, and V. Backman, Opt. Lett. **31**, 389 (2006).
[4] S. Yang, and V. N. Astratov, Appl. Phys. Lett. **92**, 261111 (2008).
[5] E. Shamonina, V. Kalinin, K. Ringhofer, and L. Solymar, Electron. Lett. **38**, 371 (2002).
[6] E. Shamonina, V. Kalinin, K. Ringhofer, and L. Solymar, J. Appl. Phys. **92**, 6252 (2002).
[7] M. Wiltshire, E. Shamonina, I. Young, and L. Solymar, Electron. Lett. **39**, 215 (2003).
[8] E. Shamonina and L. Solymar, J. Phys. D **37**, 362 (2004).
[9] M. J. Freire, R. Marqués, F. Medina M. A. G. Laso, and F. Martín, Appl. Phys. Lett. **85**, 4439 (2004).
[10] C. Zhu, H. Liu, S. M. Wang, T. Li, J. X. Cao, Y. J. Zheng, L. Li, Y. Wang, S. N. Zhu, and X. Zhang, Opt. Express **18**, 26268 (2010).
[11] H. Liu and S. Zhu, Laser Photon. Rev. **7**, 882 (2013).
[12] M. Quinten, A. Leitner, J. R. Krenn, and F. R. Aussenegg, Opt. Lett. **23**, 1331 (1998).
[13] J. R. Krenn, A. Dereux, J. C. Weeber, E. Bourillot, Y. Lacroute, J. P. Goudonnet, G. Schider, W. Gotschy, A. Leitner, F. R. Aussenegg, and C. Girard, Phys. Rev. Lett. **82**, 2590 (1999).

[14] M. L. Brongersma, J. W. Hartman, and H. A. Atwater, Phys. Rev. B **62**, R16356 (2000).
[15] S. A. Maier, M. L. Brongersma, P. G. Kik, S. Meltzer, A. A. G. Requicha, and H. A. Atwater, Adv. Mater. **13**, 1501 (2001).
[16] S. A. Maier, P. G. Kik, and H. A. Atwater, Appl. Phys. Lett. **81**, 1714 (2002).
[17] S. A. Maier, P. G. Kik, and H. A. Atwater, Phys. Rev. B **67**, 205402 (2003).
[18] S. Y. Park and D. Stroud, Phys. Rev. B **69**, 125418 (2004).
[19] W. H. Weber and G. W. Ford, Phys. Rev. B **70**, 125429 (2004).
[20] R. Shore and A. Yaghjian, Electron. Lett. **41**, 578 (2005).
[21] A. B. Evlyukhin, and S. I. Bozhevolnyi, Laser. Phys. Lett. **3**, 396 (2006).
[22] S. Wang, J. Xiao, and K. Yu, Opt. Commun. **279**, 384 (2007).
[23] V. Lomakin, M. Lu, and E. Michielssen, Opt. Express **15**, 11827 (2007).
[24] A. Alù, P. A. Belov, and N. Engheta, Phys. Rev. B **80**, 113101 (2009).
[25] A. Alù and N. Engheta, New J. Phys. **12**, 013015 (2010).
[26] M. Conforti and M. Guasoni, J. Opt. Soc. Am. B **27**, 1576 (2010).
[27] A. Alù, P. A. Belov, and N. Engheta, New J. Phys. **13**, 033026 (2011).
[28] P. J. Compaijen, V. A. Malyshev, and J. Knoester, Phys. Rev. B **87**, 205437 (2013).
[29] P. A. Belov and C. R. Simovski, Phys. Rev. E **72**, 036618 (2005).
[30] S. A. Maier and H. A. Atwater, J. Appl. Phys. **98**, 011101 (2005).
[31] K. B. Crozier, E. Togan, E. Simsek, and T. Yang, Opt. Express **15**, 17482 (2007).
[32] T. Yang and K. B. Crozier, Opt. Express **16**, 8570 (2008).
[33] X. Cui and D. Erni, J. Opt. Soc. Am. A **25**, 1783 (2008).
[34] A. A. Govyadinov and V. A. Markel, Phys. Rev. B **78**, 035403 (2008).
[35] D. S. Citrin, Opt. Lett. **31**, 98 (2006).
[36] H. Zhang and H.-P. Ho, Opt. Express **18**, 23035 (2010).
[37] P. Holmstrom, L. Thylen, and A. Bratkovsky, Appl. Phys. Lett. **97**, 073110 (2010).
[38] A. B. Evlyukhin, C. Reinhardt, A. Seidel, B. S. Luk'yanchuk, and B. N. Chichkov, Phys. Rev. B **82**, 045404 (2010).
[39] A. E. Krasnok, A. E. Miroshnichenko, P. A. Belov, and Y. S. Kivshar, Opt. Express **20**, 20599 (2012).
[40] B. Rolly, B. Stout, and N. Bonod, Opt. Express **20**, 20376 (2012).
[41] J. A. Schuller, R. Zia, T. Taubner, and M. L. Brongersma, Phys. Rev. Lett. **99**, 107401 (2007).
[42] L. Peng, L. Ran, H. Chen, H. Zhang, J. A. Kong, and T. M. Grzegorczyk, Phys. Rev. Lett. **98**, 157403 (2007).
[43] K. Vynck, D. Felbacq, E. Centeno, A. I. Căbuz, D. Cassagne, and B. Guizal, Phys. Rev. Lett. **102**, 133901 (2009).
[44] A. I. Kuznetsov, A. E. Miroshnichenko, Y. H. Fu, Z. JingBo, and B. S. Luk'yanchuk, Sci. Rep. **2**, 492 (2012).
[45] A. B. Evlyukhin, S. M. Novikov, U. Zywietz, R. L. Eriksen, C. Reinhardt, S. I. Bozhevolnyi, and B. N. Chichkov, Nano Lett. **12**, 3749 (2012).
[46] M. Law, D. J. Sirbuly, J. C. Johnson, J. Goldberger, R. J. Saykally, and P. Yang, Science **305**, 1269 (2004).
[47] C. Kopp, S. Bernabé, B. Bakir, J.-M. Fedeli, R. Orobtchouk, F. Schrank, H. Porte, L. Zimmermann, and T. Tekin, IEEE J. Sel. Top. Quantum Electron. **17**, 498 (2011).
[48] R. Quidant, J.-C. Weeber, A. Dereux, D. Peyrade, C. Girard, and Y. Chen, Phys. Rev. E **65**, 036616 (2002).
[49] P.-G. Luan, K.-D. Chang, Opt. Express **14**, 3263 (2006).
[50] G. S. Blaustein, M. I. Gozman, O. Samoylova, I. Ya. Polishchuk, and A. L. Burin, Opt. Express **15**, 17380 (2007).
[51] K.-Y. Lee, C. N. Chen, and Y. J. Lin, Opt. Quantum Electron. **40**, 633 (2008).
[52] M. I. Gozman, I. Ya. Polishchuk, and A. L. Burin, Phys. Lett. A **372**, 5250 (2008).
[53] J. Du, S. Liu, Z. Lin, J. Zi, and S. T. Chui, Phys. Rev. A **79**, 051801 (2009).
[54] R. Zhao, T. Zhai, Z. Wang, and D. Liu, J. Lightwave Technol. **27**, 4544 (2009).
[55] J. Du, S. Liu, Z. Lin, J. Zi, and S. T. Chui, Phys. Rev. A **83**, 035803 (2011).
[56] J. Du, Z. Lin, S. T. Chui, W. Lu, H. Li, A. Wu, Z. Sheng, J. Zi, X. Wang, S. Zou *et al.*, Phys. Rev. Lett. **106**, 203903 (2011).
[57] R. A. Shore and A. D. Yaghjian, Radio Sci. **47**, RS2014 (2012).
[58] R. A. Shore and A. D. Yaghjian, Radio Sci. **47**, RS2015 (2012).
[59] C. M. Linton, V. Zalipaev, and I. Thompson, Wave Motion **50**, 29 (2013).
[60] G. W. Mulholland, C. F. Bohren, and K. A. Fuller, Langmuir **10**, 2533 (1994).
[61] O. Merchiers, F. Moreno, F. González, and J. M. Saiz, Phys. Rev. A **76**, 043834 (2007).
[62] J. M. Borwein, M. L. Glasser, R. C. McPhedran, J. G. Wan, and I. J. Zucker, *Lattice Sums Then and Now* (Cambridge University Press, Cambridge, UK, 2013).
[63] J. Stratton, *Electromagnetic Theory* (McGraw-Hill, New York, 1941).
[64] E. Palik, *Handbook of Optical Constants of Solids* (Academic Press, Boston, 1985).
[65] P. Belov, S. Maslovski, K. Simovski, and S. Tretyakov, Tech. Phys. Lett. **29**, 718 (2003).
[66] S. G. Johnson and J. D. Joannopoulos, Opt. Express **8**, 173 (2001).
[67] A. B. Evlyukhin, C. Reinhardt, and B. N. Chichkov, Phys. Rev. B **84**, 235429 (2011).
[68] S. M. R. Z. Bajestani, M. Shahabadi, and N. Talebi, J. Opt. Soc. Am. B **28**, 937 (2011).
[69] A. M. Serebrennikov, Opt. Commun. **284**, 5043 (2011).
[70] B. Rolly, N. Bonod, and B. Stout, J. Opt. Soc. Am. B **29**, 1012 (2012).
[71] CST Microwave Studio 2013, CST GmbH, www.cst.com.
[72] V. Yannopapas and N. V. Vitanov, Phys. Rev. B **74**, 193304 (2006).
[73] X.-X. Liu and A. Alù, Phys. Rev. B **82**, 144305 (2010).
[74] D. Solis, B. Willingham, S. L. Nauert, L. S. Slaughter, J. Olson, P. Swanglap, A. Paul, W.-S. Chang, and S. Link, Nano Lett. **12**, 1349 (2012).
[75] D. Solis, A. Paul, J. Olson, L.S. Slaughter, P. Swanglap, W.-S. Chang, and S. Link, Nano Lett. **13**, 4779 (2013).
[76] A. B. Evlyukhin, C. Reinhardt, E. Evlyukhin, and B. N. Chichkov, J. Opt. Soc. Am. B **30**, 2589 (2013).